UCRL-TR-228409

LAWRENCE
LIVERMORE
NATIONAL
LABORATORY

High Brightness, Laser-Driven X-ray Source for Nanoscale Metrology and Femtosecond Dynamics

C. W. Siders, J. K. Crane, V. Semenov, S. Betts, B. Kozioziemski, K. Wharton, S. Wilks, T. Barbee, B. Stuart, D. E. Kim, J. An, C.P.J. Barty

February 27, 2007

This work was performed under the auspices of the U.S. Department of Energy by University of California, Lawrence Livermore National Laboratory under Contract W-7405-Eng-48.

FY06 LDRD Final Report
High Brightness, Laser-Driven X-ray Source for Nanoscale Metrology and Femtosecond Dynamics
LDRD Project Tracking Code: 04-ERD-064
Craig W. Siders, Principal Investigator

Abstract

This project developed and demonstrated a new, bright, ultrafast x-ray source based upon laser-driven K-alpha generation, which can produce an x-ray flux 10 to 100 times greater than current microfocus x-ray tubes. The short-pulse (sub-picosecond) duration of this x-ray source also makes it ideal for observing time-resolved dynamics of atomic motion in solids and thin films.

Introduction/Background

With the development of high-intensity, ultrafast, table-top laser systems based upon chirp pulse amplification (CPA)[1], intense sources of x-rays from laser-solid target interactions were discovered[2-4]. K-alpha emission from solid targets has already proven to be a useful and suitably bright source for ultrafast, time-resolved x-ray diffraction[5, 6]. To produce bright, K-alpha x-rays, an ultrafast, high-intensity laser is focused onto a solid target. If a sufficient prepulse exists ~0.1-1 ns before the main laser pulse, a dense plasma is formed and expands outward from the metal surface. This preplasma is a dense source of electrons that are then accelerated by the ponderomotive force of the main laser pulse to energies on the order of the ponderomotive potential, U_p, given by:

$$U_p[\text{eV}] = 9.33\text{X}10^{-14}\ I\ [\text{W/cm}^2]\ \lambda^2[\mu\text{m}] \qquad (1)$$

where I is the focused laser intensity and λ is the laser wavelength, 0.8 μm for Ti:Sapphire and 1044-nm for our Yb-fiber ultrashort system. At 10^{18} W/cm^2 these plasma electrons are accelerated to ~60 KeV and have a high probability for exciting K-shell transitions in transition metals such as Cu and Ga, producing bright x-ray line emission of several kilovolts. If the drive laser is tightly focused onto the metal surface a very small emittance area (few microns), a high-brightness source of K-alpha radiation can be produced.

Applications

One of the hottest areas in physical science is sub-picosecond time-resolved dynamics of atomic, molecular, and solid-state systems [7, 8]. By combining the intrinsic, ultrafast (<100 fs) duration of this K-alpha x-ray source with the Lab's capability to produce efficient x-ray optics we propose to develop a unique tool for studying sub-picosecond, phenomena over submicron scale lengths. The sub-micron dimension of the focused x-ray probe allows localized interrogation of the sample, or diagnostics on very small samples such as macromolecules. On the time scales of 100 fs to 10's of ps we should be able to characterize a wide variety of physical processes such as electron-photon coupling, inter-atomic motion, molecular bending, folding, and fragmentation, which in turn will enable a wide range of potential uses in chemistry, surface science, biology, and nanotechnology.

Currently there is no satisfactory method for rapidly characterizing the frozen hydrogen layer inside a Be shell NIF target. This type of in-situ imaging is essential for diagnosing imperfections such as voids or cracks in the hydrogen ice that would seriously impact the results of a NIF cryo-ignition shot. In recent studies by Bernie Kozioziemski [9] et.al, they describe the use of x-ray, phase-contrast radiography to measure the hydrogen ice-layer on the inside of the Be shell of the NIF targets. Figure 1 shows an example of such a target phase-contrast image taken with a microfocus x-ray tube. Phase contrast imaging is a technique originally developed to characterize biological samples [10] and other systems that are weakly absorbing to the x-rays. The technique relies on the high spatial coherence produced from a very small source and so is a good match for our laser-driven K-α source. A key advantage of our source over conventional microfocus tubes will be the reduced exposure time (minutes to seconds) for producing the type of image shown in Fig. 1. Eventually this may allow in-situ characterization of targets immediately prior to a NIF ignition shot.

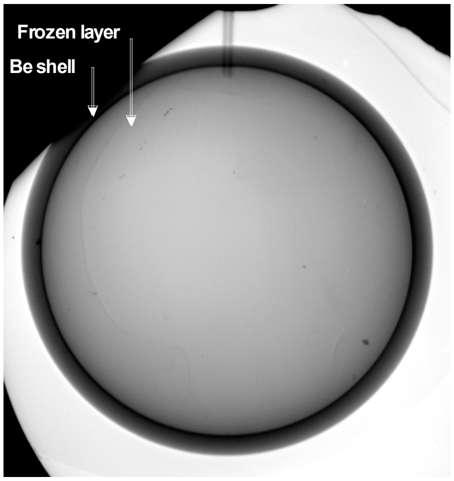

Figure 1 X-ray radiograph shows NIF cryo-target taken with x-ray tube:several minute exposure.

Research Activities

For the first year, FY04, we assembled the vacuum equipment, set-up the experiment at the output of a small grating compressor in the Falcon Laser Lab, and characterized the laser pulse in energy, duration, and spatial extent in order to characterize the focal irradiance at the target. We designed and manufactured a vacuum-compatible Cu-tape drive source that continuously feeds new material to the interaction region, shown in Fig.2.

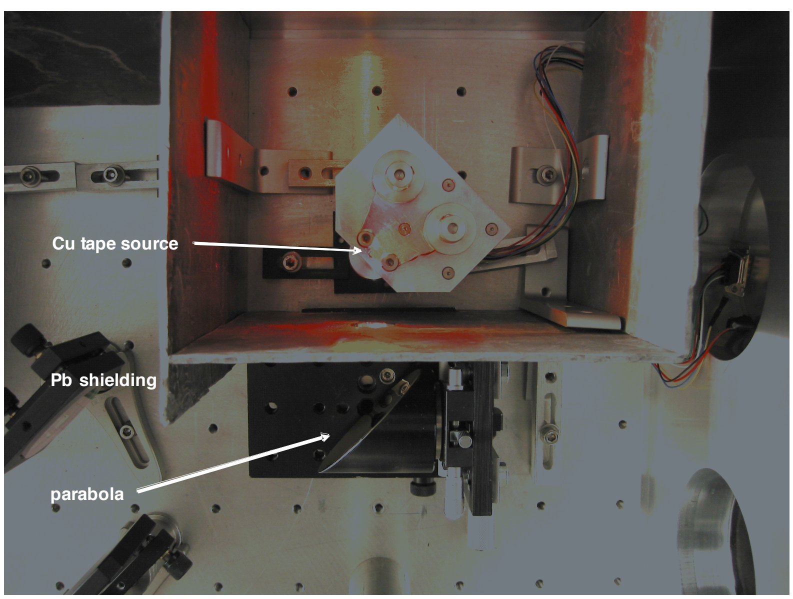

Figure 2. Copper source for x-ray generation is housed in vacuum vessel and surrounded by Pb sheet to reduce the background of scattered x-rays.

Another accomplishment in the first year was to develop a model to help optimize the production of copper K-alpha x-rays by manipulating the laser energy, prepulse, copper target thickness and laser spot size. The model was developed by Scott Wilks, one of our collaborators. The first part of the model uses an atomic physics code, LSP, that contains all the rates and cross sections for electron impact excitation, Auger decay, and spontaneous emission. The second part of the model uses a Monte Carlo transport code, ITS, to track the transport of the hot electrons and x-ray photons in the material.

At the end of FY04 and early FY05 we performed a series of experiments to characterize the production of Cu K-alpha x-rays as a function of various laser and target parameters. The laser target configuration is shown in Fig. 3. The laser is focused with an f/3, off-axis parabola onto the moving Cu tape target. X-rays, emitted in the forward direction transmit through a hole in the Pb shielding and then through two Be vacuum windows to an x-ray ccd camera mounted outside of the vacuum chamber. We adjust the energy over a range of 1.5 mJ to 15 mJ, producing a focal irradiance of $6X10^{16}$ W/cm^2 to $6X10^{17}$ W/cm^2 for a target oriented normal to laser propagation. For most cases we orient the target (Cu foil) at 45 degrees with the laser p-polarized to get the maximum efficiency for x-ray generation. To get an absolute calibration of the x-ray CCD we measure an Fe55 source of known activity.

Figure 3 shows a measurement of the K-alpha x-ray yield as a function of position of the target plane with respect to the laser focus, located at z = -80 microns. The x-ray yield is lowest near the laser focus where the laser irradiance is highest. Away from focus, where the spot size is larger reducing the focal irradiance the x-ray yield goes up. In the second plot we show yield as a function of laser energy with the target positioned at best focus. The highest yield is at an energy of 1.5 mJ, which gives an irradiance of $4.3X10^{16}$ W/cm^2. These results are in qualitative agreement with the work of Reich et.al., [11] where they found a scaling relationship for optimal laser irradiance for K-alpha production of,

$$I_{opt} = 7 \text{ X } 10^9 \, Z^{\,4.4}, \qquad (2)$$

which for Cu (Z=29), gives a value of I_{opt} = $2.0X10^{16}$ W/cm^2, and an electron temperature scaling relationship,

$$kT \sim 130 \text{ keV Sqrt}\{I / 10^{17} \text{ W cm-}^2\} \qquad (3)$$

At larger values of laser irradiance the electron temperature increases to a value where the efficiency for generating K-holes in Cu goes down and the K-alpha emission is reduced. Since our goal is to generate the smallest x-ray emitter possible the region of best laser focus is where we want to operate.

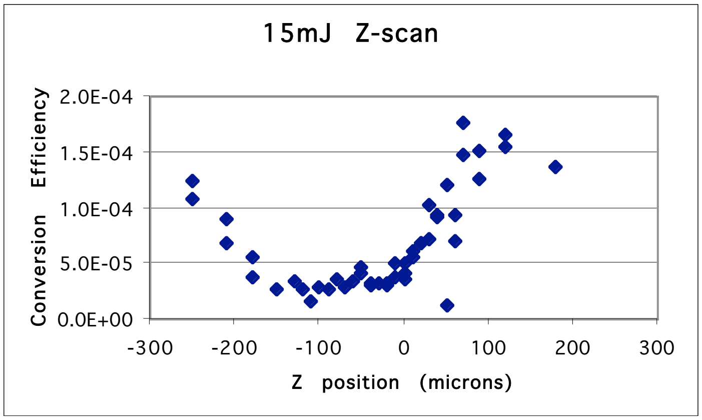

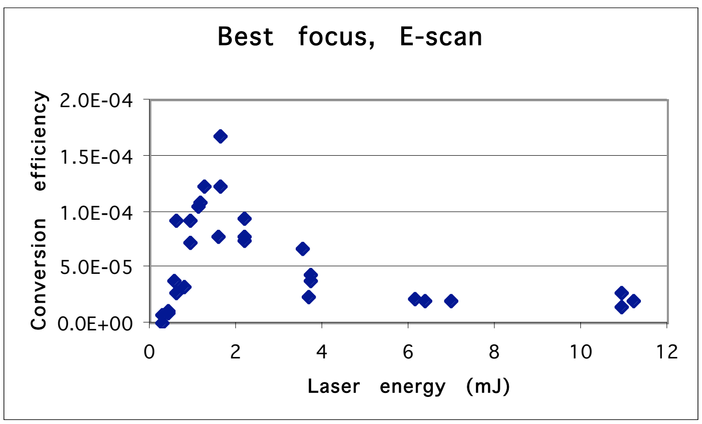

Figure 3. (top) X-ray conversion efficiency vs z position of target for the highest irradiance laser shots, $6X10^{17}$ W/cm^2; X-ray conversion efficiency vs energy at best focus.

The x-ray emitter size was measured using the knife-edge technique. This measurement with the Falcon laser (Ti:S) setup at 800 nm, yielding a 10-um spot size, with considerable impact from tape motion – an issue which would be alleviated used a liquid jet target.

The geometrical behavior of the x-ray flux was systematically studied using the ITS Tiger Monte-Carlo codes. Figure 4 shows a demonstrative example of the x-ray yield in 3D for a 250-um copper wire. In this model, monoenergetic electrons were sent normal to the surface of the wire, and the K-alpha emission in different directions was obtained. As expected, at energies significantly below approximately three times the K-edge produced little flux. From 60-keV to 600-keV, x-ray emission was limited to only one side of the wire due to re-adsorption of the x-rays in the bulk of the wire. At 1-MeV and above, significant x-ray flux in the forward direction is obtained.

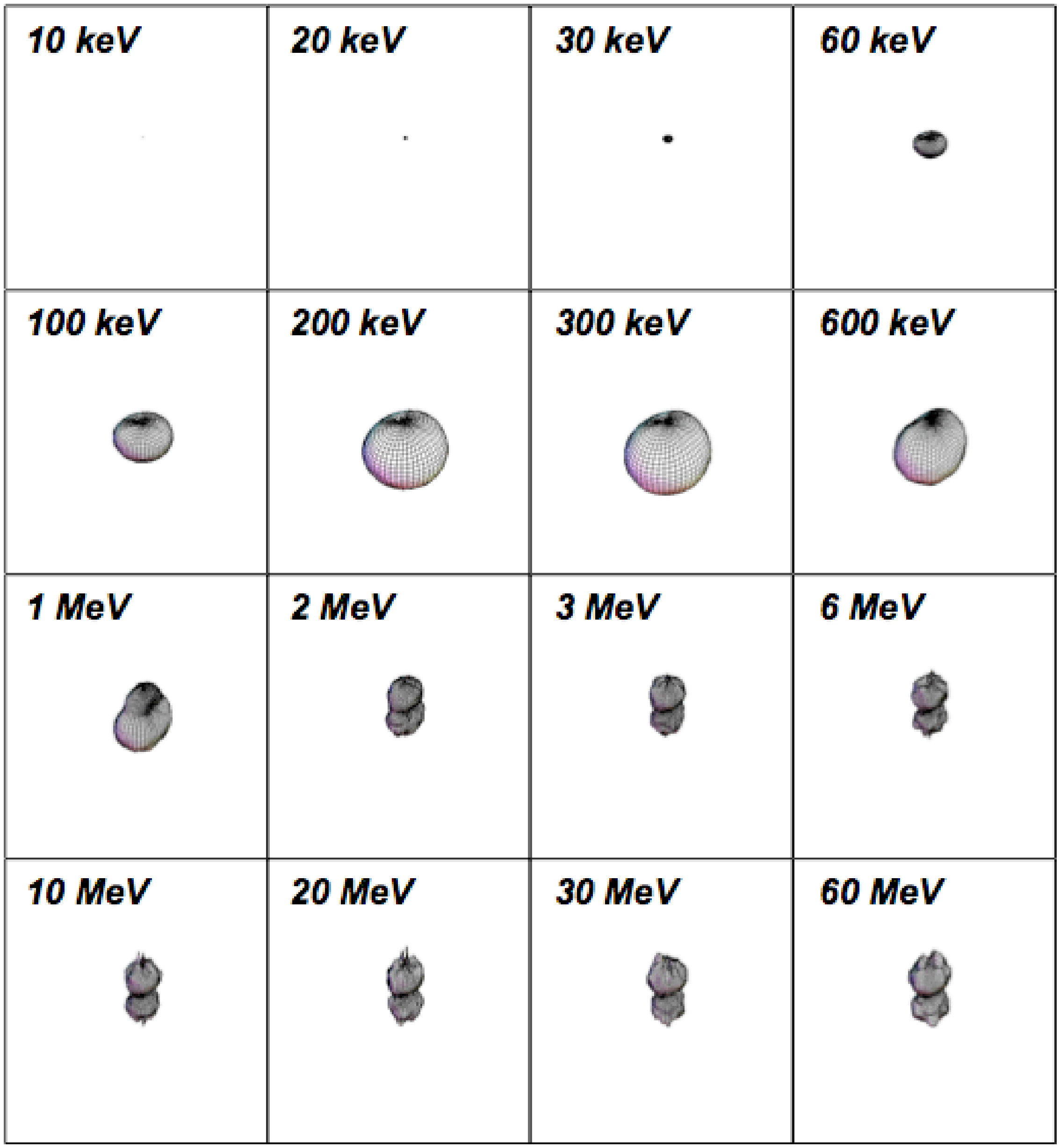

Figure 4. X-ray conversion efficiency vs direction in 3D for a cylindrical Cu wire target, as a function of incident mono-energetic electron energy. The wire (not shown explicitly in the figures) runs approximately horizontally and is most clearly located for the 1-MeV case. The electron beam is oriented vertically, with electrons directed up in the figures. Results obtained using the ITS TIGER codes.

In the final year of this project, primary effort was put towards the integration of the K-alpha source with a high rep-rate Yb:fiber chirped pulse amplified laser system, which was constructed as part of Jay Dawson's parallel effort (04-ERD-048). Secondarily, a design study was performed to predict the x-ray flux attainable, with small spot size, with such compact fiber-based systems.

Optimization of the x-ray source requires operating at a peak intensity given by Equation 2, above. With an application-driven requirement of small spot size (e.g. conventional micro-focus x-ray tubes have an ~5-um source size), this becomes a required peak power – for Cu or Ga and a 5-um spot size, this the required peak power is 3.7-GW. To achieve this level of peak compressed-pulse power, a novel pulse stretcher had to be designed and constructed as part of this project. To obtained highest output energy, this stretcher had to provide a long (multi-nanosecond) stretched pulse width, and to allow compression to as short a pulse duration as possible a wide bandwidth needed to be maintained (a 20-nm bandwidth was used in the design and slightly shorter than this was realized in the laboratory). A 1780-groove/mm high efficiency multi-layer dielectric grating was used in a tightly folded configuration (see figure 5) based upon the Lemoff and Barty design [12]. A traditional Treacy two-grating compressor was used, though folded with a horizontal roof mirror to use only one 20-cm wide 1780 groove/mm grating.

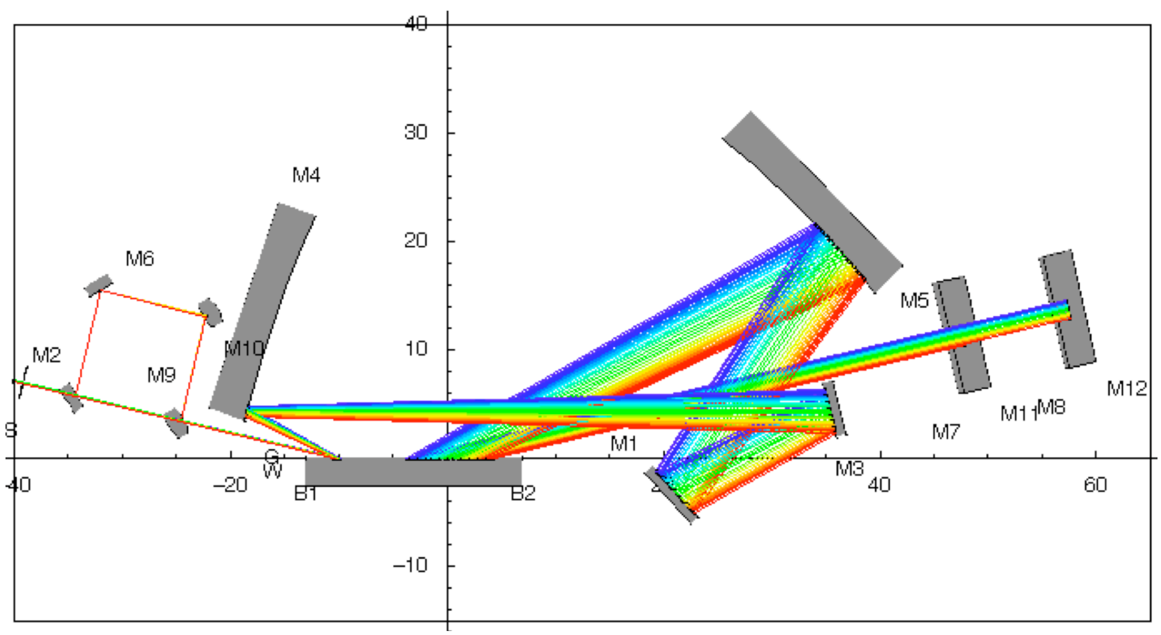

Figure 5. The folded, single 1780-groove/mm grating stretcher designed and built for seeding a Yb:fiber CPA system. A 76.5-deg angle of incidence was used and for a 1044-nm center wavelength, the GDD is 5.4×10^{7} fs^2, the TOD -7.5×10^{8} fs^3, the fourth order 1.7×10^{10} fs^4, and the fifth order -5.5×10^{11} fs^5.

A detailed model for the dispersion of the entire fiber laser system was created, including the ray-trace obtained dispersion of the stretcher and compressor, and the individual fiber amplifier sections. For the latter, the effects of waveguide dispersion in the fibers was fully included. A system operating point was chosen that theoretically had less than 200-fs of residual group delay across the full 20-nm design bandwidth.

Our Yb:fiber CPA system operated with 1044-nm center wavelength and as high as 300-uJ output energy and ~50-kHz operation, though not simultaneously as available laser diode pump power was insufficient. Typical operating values for x-ray generation experiments were 100-uJ and 5-kHz (limited by the speed of the Cu tape target). Pulse duration was a key issue, as the shortest recompressed pulse length was ~350-fs FWHM, or a 300-MW peak power – significantly lower than the optimum 3.7-GW for efficient x-ray generation discussed above for a 5-um spot size. Using a tight-focus objective, though, a 1.8-um FWHM focal spot was measured – indicative of the excellent beam quality obtained from the fiber amplifiers – and hence a peak theoretical intensity of 1.1×10^{16} W/cm^2 (only 3x less than the optimum intensity for Cu) would be possible.

X-Ray yield experiments were performed using both a single-hit x-ray CCD camera and a Si x-ray PIN photodiode from Amptek. Care was taken to orient the x-ray source as close to the Be exit window as possible to maximize collected solid angle on the detector. No x-ray signal was seen above background levels. A systematic scan of compressor angle-of-incidence was performed to ensure that the optimal angle for shortest pulse was used, with still no x-rays observed. At the last week of the project's schedule, the focal intensity was checked by looking for short-pulse ionization of air, which occurs at an intensity of 4×10^{14} W/cm^2. This provided an independent estimate of the "effective pulse width" of 2-3 ps – i.e. the pulsewidth which is consistent with the measured pulse energy, focal spot size, and over-factor for air breakdown (our peak intensity was 5x above the threshold). At the conclusion of the experiment campaign, it could not be concluded what in the laser system accounted for the incompressibility of the output pulse. Later FROG-based measurements of the output pulse indicated an anonymously large higher-order phase, predominately fourth order phase of approximately 10^9 fs^4. Future efforts will directly characterize the spectral phase using FROG and use phase precompensation methods.

FLEX X-Ray Source Scalings

Future applications of compact short-pulse fiber laser-driven K-alpha sources can benefit in two ways from the higher average laser power achievable compared to traditional bulk Ti:Sapphire lasers (see figure 6). First, simply by reducing the time to acquire x-ray images or diffraction patterns, new capabilities are accessed – e.g systematic material system studies are possible where before only limited representative cases could be examined. Secondly, by enabling the acquisition of x-ray data on significantly more dis-ordered materials in reasonable times (as indicated by the "pain threshold" in the figure), new science can be accessed.

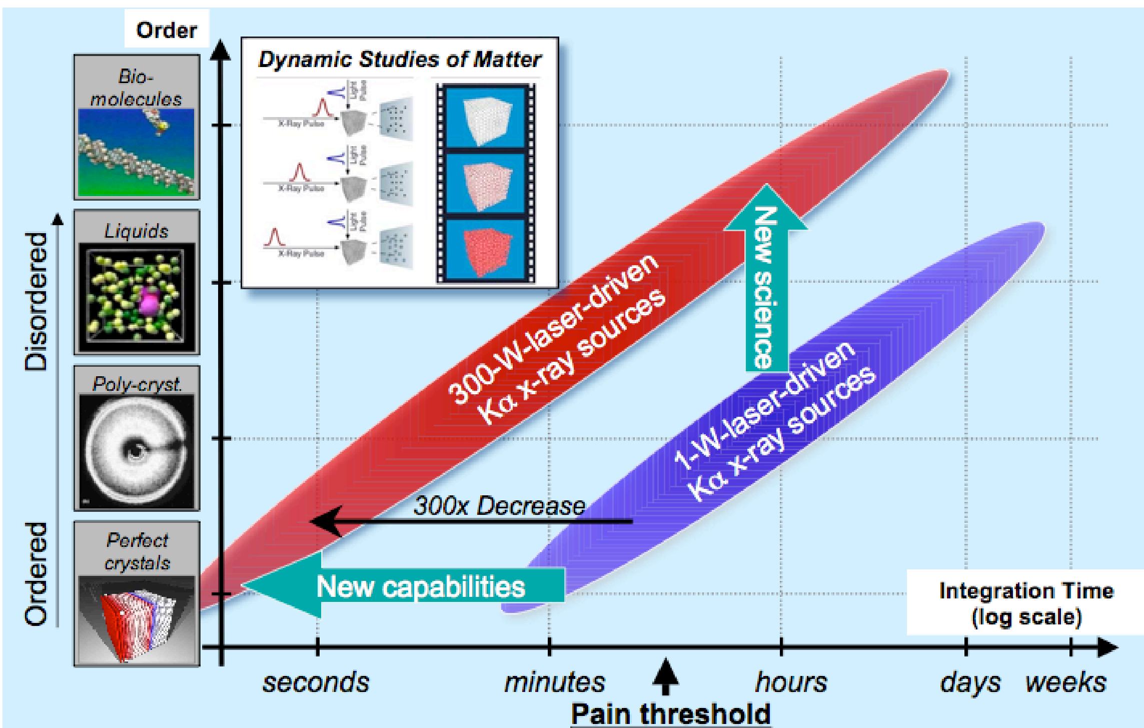

Figure 6. High-average power driven k-alpha sources (red ellipse) have two distinct impacts: accessing new capabilities in well-ordered materials studies through reduction in integration time, and accessing new science by enabling the study of less ordered materials in acceptable integration times.

To quantify the potential increase in flux achievable, a study was performed to compare a traditional micro-focus x-ray tube (a Thomson Kevex PXS927-EA, with 5-um resolution) with a laser-driven k-alpha source. The results of Reich [11] were used to model the conversion of incident laser light to a Maxwellian electron energy distribution. Integration of this distribution over a photon yield curve provide the total x-ray flux. Photon yield curves were obtained not only from Reich, but by ITS-TIGER Monte-Carlo modeling of several target materials/configurations of interest. These include 250-um wire and slab Cu, 30-um Ga jet, and 250-um Kr jet. Photon yield versus electron energy are shown in figure 7, along with the literature results from Dick et al. [13] for Cu K-alpha on bulk targets. The experimentally measured yield for a Thomson-Kevex tube are shown for comparison.

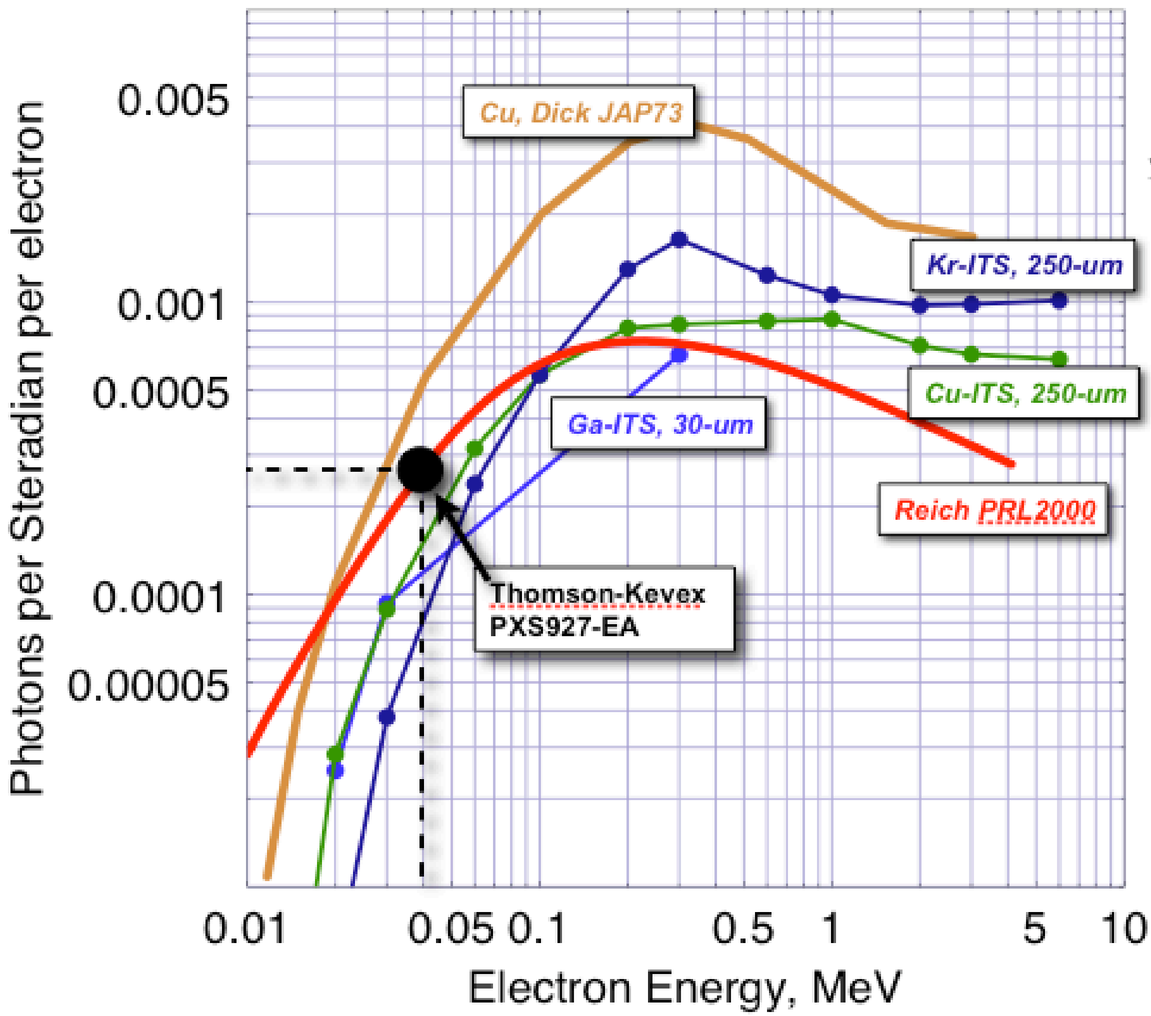

Figure 7. Photon yield (K-alpha photons per steradian per electron) versus incident electron energy for bulk Cu (Dick [13]), 250-um Cu wire, 30-um Ga, 250-um Kr, and the empirical result obtained from Monte Carlo runs on bulk Cu in Reich.

Finally, assuming a 5-um spot size and optimal peak power/intensity (3.7 GW in this case), figure 8 compares the expected laser-driven x-ray flux with the space-charge limited flux from the Kevex tube. Above 25-W average laser power, the laser-driven Cu k-alpha source shown here would exceed the flux of a micro-focus x-ray tube. Upper limits on rep-rate imposed by either the target or laser (most significantly the acousto-optic modulators which can be driven at a few hundred kilo-hertz) limit the maximum achievable flux to approximately 40x the tube value.

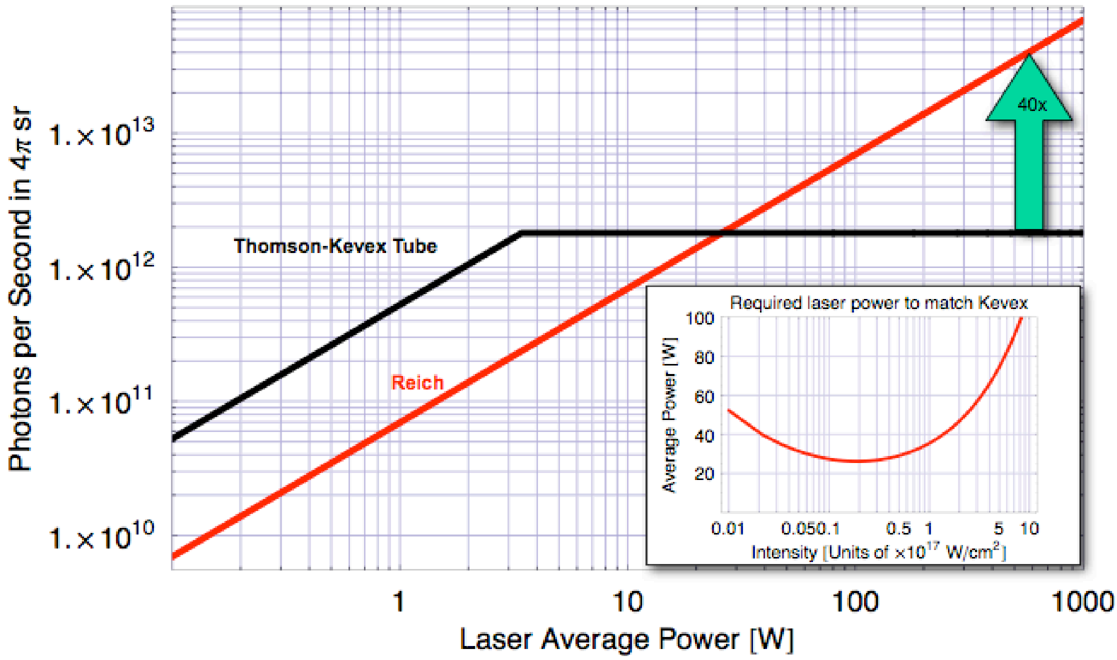

Figure 8. Estimated photon flux (photons per second into all directions) for a laser-driven Cu K-alpha x-ray source versus laser average power on target. Peak focal intensity on the assumed 5-um spot is kept at the optimum value for efficient x-ray generation. For comparison, a Thomson-Kevex tube is shown, which can supply up to the indicated flux at 3.5-W electrical drive power. Above 25-W laser power, the laser-driven source exceeds the micro-focus tube power. Practical limits of target replenishment and laser rep-rate will clamp average power achievable to the sub-kW level, indicating an approximate 40x upper limit on x-ray flux improvement.

Exit Plan

Two exit plans are envisioned for this work. Firstly, based upon this LDRD's results, a fiber laser driven Ga jet/droplet K-alpha source is in consideration as a replacement for the micro-focus x-ray sources used on NIF target diagnostics. Providing even 10x reduction in integration time would enable capsule preparations based upon quick cooling just prior to a shot. Secondly, interest in the ultrafast x-ray community for higher-flux sources is growing, as is interest in the FLEX source and its capabilities. Discussions with both the Center for Integrative Nano-Technology and the Advanced Photon Source for collaborative DOE BES proposals are ongoing.

Acknowledgements

The authors would like to acknowledge the significant contributions of J. Price, D-E. Kim, and J. An during their visits to LLNL.

References

[1] D. Strickland and G. Mourou, "Compression of Amplified Chirped Optical Pulses," *Opt. Commun.*, vol. 56, pp. 219-221, 1985.

[2] J. C. Kieffer, M. Chaker, J. P. Matte, H. Pepin, C. Y. Cote, Y. Beaudoin, T. W. Johnston, C. Y. Chien, S. Coe, G. Mourou, and O. Peyrusse, "Ultrafast X-ray sources," 1993.

[3] J. D. Kmetec, C. L. Gordon, III, J. J. Macklin, B. E. Lemoff, G. S. Brown, and S. E. Harris, "MeV X-ray generation with a femtosecond laser," *Phys. Rev. Lett.*, vol. 68, pp. 1527-30, 1992.

[4] M. M. Murnane, H. C. Kapteyn, M. D. Rosen, and R. W. Falcone, "Ultrafast X-ray pulses from laser-produced plasmas," *Science*, vol. 251, pp. 531-6, 1991.

[5] C. Rischel, A. Rousse, I. Uschmann, P. A. Albouy, J. P. Geindre, P. Audebert, J. C. Gauthier, E. Forster, J. L. Martin, and A. Antonetti, "Femtosecond time-resolved X-ray diffraction from laser-heated organic films," *Nature*, vol. 390, pp. 490-2, 1997.

[6] C. Rose-Petruck, R. Jimenez, T. Guo, A. Cavalleri, C. W. Siders, F. Raksi, J. A. Squier, B. C. Walker, K. R. Wilson, and C. P. J. Barty, "Picosecond-milliangstrom lattice dynamics measured by ultrafast X-ray diffraction," *Nature*, vol. 398, pp. 310-312, 1999.

[7] A. Zewail, "Nobel Prize in Chemistry," 1999.

[8] A. Zewail, *J. Phys. Chem. A*, vol. 104, 2000.

[9] B. J. Kozioziemski, UCRL-JRNL-205025.

[10] S. Wilkins and e. al., *Nature*, vol. 384, pp. 335, 1996.

[11] C. Reich, P. Gibbon, I. Uschmann, and E. Forster, "Yield optimization and time structure of femtosecond laser plasma K alpha sources," vol. 84, pp. 4846-4849, 2000.

[12] B. E. Lemoff and C. P. J. Barty, "Quintic-Phase-Limited, Spatially Uniform, Expansion and Recompression of Ultrashort Optical Pulses," vol. 18: Opt. Lett, 1993, pp. 1651-1653.

[13] C. E. Dick, A. C. Lucas, J. M. Motz, R. C. Placious, and J. H. Sparrow, "Large-angle L X-ray production by electrons," *Journal of Applied Physics*, vol. 44, pp. 815-26, 1973.